Title
Electrochemolipolysis of Human Adipose Tissue

Journal
Facial Plastic Surgery & Aesthetic Medicine, 22(2)

ISSN
2689-3614

Authors
Hutchison, Dana M
Hakimi, Amir A
Hong, Ellen M
et al.

Publication Date
2020-04-01

DOI
10.1089/fpsam.2019.29011.hut

Peer reviewed

Facial Plastic Surgery & Aesthetic Medicine
Volume 22, Number 2, 2020

DOI: 10.1089/fpsam.2019.29011.hut

Facial Plastic Surgery & Aesthetic Medicine

ORIGINAL INVESTIGATION

Electrochemolipolysis of Human Adipose Tissue

Dana M. Hutchison, MS,[1] Amir A. Hakimi, BS,[1] Ellen M. Hong, BA,[1] Tiffany T. Pham, MD,[1] Avin Wijayaweera,[1] Soohong Seo, MD,[2] Yueqiao Qu, PhD,[1] Melissa Bircan,[1] Ryan Sivoraphonh,[1] Brandyn Dunn, MD, MPH,[3] Chung-Ho Sun, PhD,[1] Mark R. Kobayashi, MD,[4] Sehwan Kim, PhD,[5] and Brian J.F. Wong, MD, PhD[1,3,6,*]

Abstract

Importance: Body fat contouring procedures have increasingly grown in popularity over the years. As such, there is a need for inexpensive, minimally invasive, and simple fat reduction/contouring technique.

Objective: To examine the acid–base and histological changes in ex vivo human adipose tissue after electrochemolipolysis (ECL).

Design, Setting, and Participants: Panniculus tissue specimens obtained after abdominoplasty procedures were tumesced with normal saline. Two platinum needle electrodes were inserted into each sample and connected to a DC power supply. Voltage (3–6 V) was varied and applied for 5 min. Specimens were sectioned through a sagittal midline across both electrode insertion sites and immediately stained with pH-sensitive dye. A numerical algorithm was used to calculate the area of the dye color change for each dosimetry pair. Samples were also evaluated utilizing light microscopy (hematoxylin and eosin). An ex vivo human adipose tissue model was used for evaluating the effects of ECL.

Results: Acidic and basic pH was appreciated surrounding the anode and cathode insertion sites, respectively. The effect was spatially localized and dose dependent. Statistical analysis of these data showed no significant difference between the mean area of the pH disturbance generated at the anode compared with the cathode at 3 V for 5 min (6.04 mm^2 vs. 2.95 mm^2, $p = 0.40$, 95% CI −4.8 to 11). A significantly greater area of pH disruption was generated at the cathode versus the anode in groups 4 V for 5 min (14.7 mm^2 vs. 5.00 mm^2, $p = 0.032$, 95% CI 0.93–19), 5 V for 5 min (15.5 mm^2 vs. 6.72 mm^2, $p = 0.019$, 95% CI 1.6–16), and 6 V for 5 min (22.5 mm^2 vs. 10.0 mm^2, $p = 0.047$, 95% CI 0.22–25). Acute structural changes in adipocytes were observed in all specimens. Vascular damage with adjacent adipocyte necrosis was prominent at the cathode site in group 6 V for 5 min.

Conclusions and Relevance: ECL at the studied dosimetry parameters induced acid and base changes in human adipose tissue, suggesting its potential use in nonsurgical fat reduction as an ultralow cost alternative to current lipolytic devices and pharmaceuticals.

Level of Evidence: NA.

Introduction

The popularity of body fat contouring procedures has grown exponentially over the past few years, with patients more frequently selecting procedures that are office based, offer shorter recovery times, and that are less invasive than traditional liposuction.[1] Contemporary minimally invasive fat reduction modalities include cryolipolysis,[2] injectable deoxycholic acid,[3] radiofrequency ablation,[4] low-level laser therapy,[5] and high-intensity focused ultrasound.[6] The common therapeutic goal underlying these technologies is targeted reduction of adipocyte cells for long-term fat volume reduction by inducing apoptosis, fat necrosis, or a combination thereof.[7] However, these modalities require the use of expensive devices or drugs and can be technically challenging to operate. As such, there is a need for inexpensive, minimally invasive, and simple

[1]Beckman Laser Institute & Medical Clinic, University of California, Irvine, Irvine, California.
[2]Department of Dermatology, Korea University Anam Hospital, Seoul, South Korea.
Departments of [3]Otolaryngology–Head and Neck Surgery and [4]Plastic Surgery, University of California, Irvine, School of Medicine, Orange, California.
[5]Beckman Laser Institute Korea, School of Medicine, Dankook University, Cheoan, Chungnam, Republic of Korea.
[6]Department of Biomedical Engineering, University of California, Irvine, Irvine, California.

*Address correspondence to: Brian J.F. Wong, MD, PhD, Beckman Laser Institute & Medical Clinic, University of California, Irvine, 1002 Health Sciences Road, Irvine, CA 92697, Email: bjwong@uci.edu

KEY POINTS

Question: How does electrochemolipolysis (ECL) therapy affect human adipose tissue?

Findings: This ex vivo human tissue study found that ECL causes spatially localized and dose-dependent pH changes within adipose tissue. Acute structural changes in adipocytes were observed in all specimens. Vascular damage with adjacent adipocyte necrosis was prominent when applying higher voltage.

Meaning: With future development, ECL may offer a low-cost minimally invasive method of destroying adipocytes for medical or cosmetic purposes.

fat reduction/contouring technique. One potential solution is a modification of electrochemical therapy hereon coined electrochemolipolysis (ECL).

ECL initiates oxidation–reduction (redox) reactions in tissue through the insertion of two passivated electrodes into a saline laden (tumescent) surgical field followed by the application of an electrical potential from a DC power supply. Electrical energy is converted into chemical energy through hydrolysis at the electrodes, with paired redox reactions occurring within the tissue: reduction of water at the cathode and oxidation at the anode. Accordingly, this reaction generates pH gradients within the tissue through the production of hydroxide ions at the cathode and hydrogen ions at the anode, leading to spatially localized biophysical alterations. Our group has previously described the potential of electrochemical therapy to reshape cartilage,[8–15] and more recently, to modify collagen in dermal skin.[16,17]

This study is the first to characterize the redox-induced alteration to ex vivo human adipose tissue. Specifically, we aim to identify structural changes that occur after these electrochemical reactions through pH landscape mapping and histopathological analysis. We hypothesize that ECL in the subcutaneous layer will trigger a series of cellular events including cell membrane lysis, saponification of triglycerides, and degradation of proteins, ultimately reducing the number and volume of adipocytes (Fig. 1).

Materials and Methods

This protocol was approved by the University of California, Irvine Institutional Review Board.

Tissue preparation

Large ($20 \times 12 \times 7$ cm) composite specimens of human skin and adipose tissue harvested from eight donors after panniculectomy procedures were wrapped in phosphate-buffered sodium-soaked gauze for a maximum of 4 hours

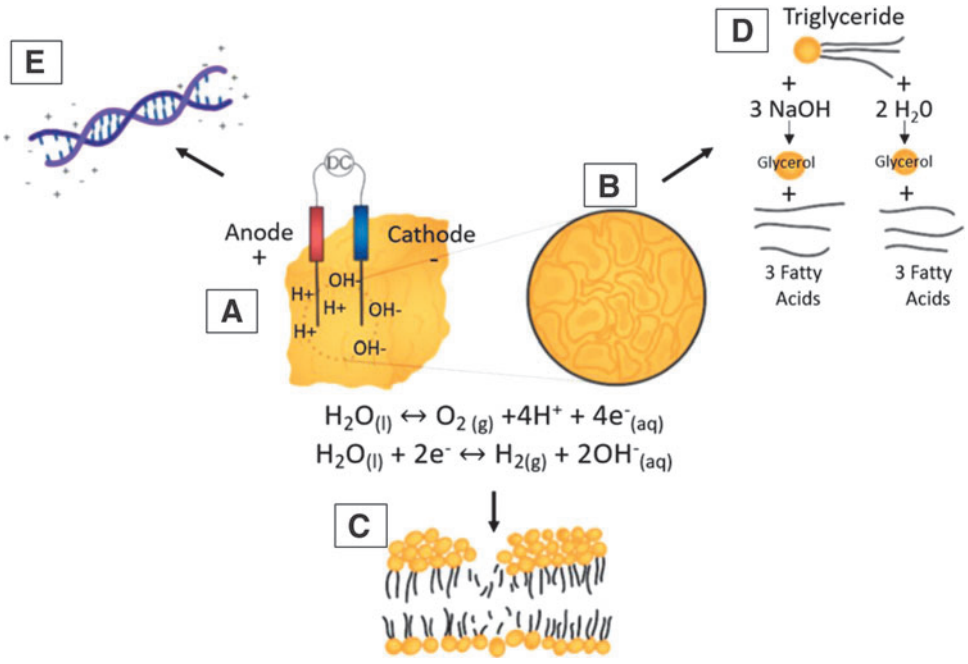

Fig. 1. ECL reaction. **(A)** Insertion of electrodes into tissue with application of electrical potential converts electrical energy to chemical energy. **(B)** Lipolysis of tissue. **(C)** Adipocyte cell membrane lysis. **(D)** Saponification of triglycerides. **(E)** Nucleic acid and protein degradation. ECL, electrochemolipolysis.

before processing to optimize viability. Samples were trimmed with a razor blade to a standard dimension of $1 \times 2 \times 1.5$ cm. Each individual section was tumesced with 3 cc of normal saline (0.9% sodium chloride) administered over six injections, providing a medium for hydrolysis and more turgid tissue to facilitate the easier insertion of electrodes.

ECL intervention

Two platinum needle electrodes (13 mm in length) were inserted perpendicular to the surface of the dermis into adipose tissue. A custom three-dimensional printed acrylic jig placed along the surface of the dermis was used to space the electrodes 3 mm apart from one another and secure them during insertion and throughout the procedure (Fig. 2). ECL was applied with current drawn from a power supply (Agilent, Santa Clara, CA) at dosimetry parameters of 3 to 6 V exposed for 5 min. These specific voltage and time parameters were selected based on unpublished pilot studies that demonstrated therapeutic potential in porcine fat. Current was applied to a total of 35 individual treatment samples (3 V: $n = 6$, 4 V: $n = 10$, 5 V: $n = 11$, 6 V: $n = 8$); no current was run through the eight control samples.

pH mapping

Specimens were hemisectioned with a razor blade along a centerline through the anode and cathode needle insertion sites. One drop of halochromic pH-sensitive dye sensitive between pH 2 and 10 (Micro Essential Lab, Brooklyn, NY) was applied to the cut surface. The immediate color change was captured with a digital single-lens reflex camera (Rebel XS EOS; Canon USA, Inc., Melville, NY), with the focus set between the electrode sites. Standardized illumination of the samples for photography was obtained by shining an LED lantern through white fabric to create diffused even lighting. A pH calibration scale and a ruled scale were included in each photograph.

A custom MATLAB algorithm was developed to quantify the area of pH perturbations at anode and cathode sites in each image and to obtain spatial pH distribution data as a function of dosimetry. Specifically, the photographs were processed using CIELAB, a color space designed to be perceptually uniform to human color vision (Supplementary Fig. S1). This algorithm permits users to determine the region-of-interest (ROI) of a select color for semiautomatic segmentation. The mean value of the ROI and the Euclidean distances between the mean and each pixel within the ROI are then calculated. Images are segmented based on the boundary created by pixel values that are 3 SDs away from the calculated mean distance. A hole filling technique is applied to remove any discontinuities. Finally, the averaged horizontal length and the area are outputted for further analysis. A two-tailed paired *t*-test was used to compare the mean area of pH alteration differences between anode and cathode sites at each treatment voltage. Statistical significance was assigned to p-values <0.05.

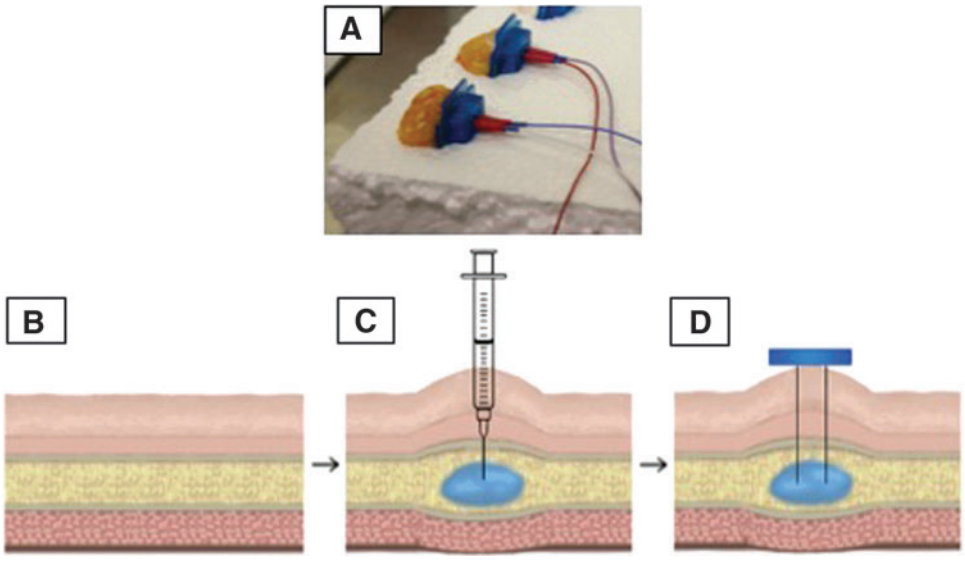

Fig. 2. Experiment design. **(A)** Styrofoam block with fat specimen held by three-dimensional printed jigs and penetrated by electrodes. **(B)** Schematic representation of human tissue. **(C)** Saline injected into adipose layer to achieve tumescence. **(D)** Electrodes inserted into tumesced adipose tissue.

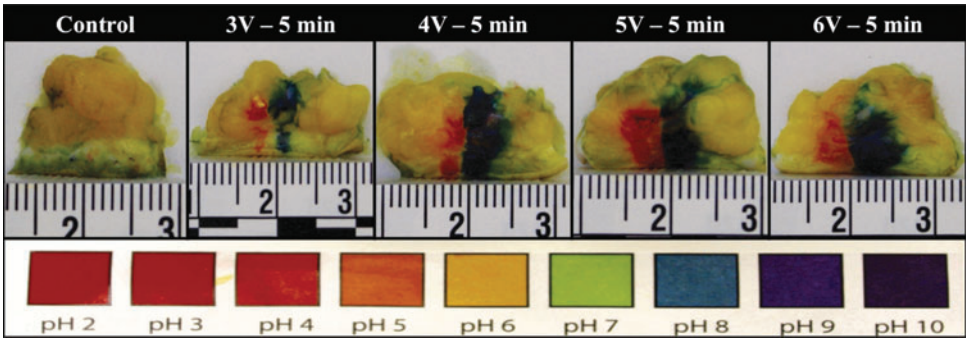

Fig. 3. ECL effect on composite human tissue with increasing voltage (V) and constant time (5 min), visualized as pH perturbation in hemisected samples. Samples are oriented with the surface of insertion site (dermis) along the bottom. Color change reflects pH alteration at anode (red) and cathode (blue) sites. Universal pH indicator chart included for reference.

Histology

Thirty-five ECL-treated samples and eight untreated control samples of composite skin and adipose tissue were fixed in 10% formalin in a 20:1 solvent-to-tissue volume ratio for a minimum of 1 week. Fixed specimens then underwent automated processing (Tissue-Tek VIP 6-A1; Sakura) according to the standard large breast tissue schedule at the University of California, Irvine Medical Center.

Sectioning was performed using a rotary microtome (HM 340 E; Swerdlick systems) with a disposable knife blade. Section thickness ranged from 6 to 10 μm. Whole-mount sections were stained with hematoxylin and eosin. A light microscope at 10×magnification captured representative images of ECL-treated sites and controls.

Results

pH mapping

ECL induced simultaneous acid–base chemical reactions at the anode and cathode sites, visualized as pH perturbation (Fig. 3). Acidic pH (red) was appreciated surrounding the anode insertion site, and basic pH (blue) was appreciated surrounding the cathode insertion site, consistent with hydrolysis and generation of hydrogen and hydroxide ions at the respective electrodes. The effect was spatially localized and dose dependent.

Automated computer software quantified the spatial extent (mm^2) of pH perturbation surrounding the anode and cathode insertion sites at each treatment voltage (Fig. 4). Statistical analysis of these data showed no significant difference between the mean area (mm^2) of the

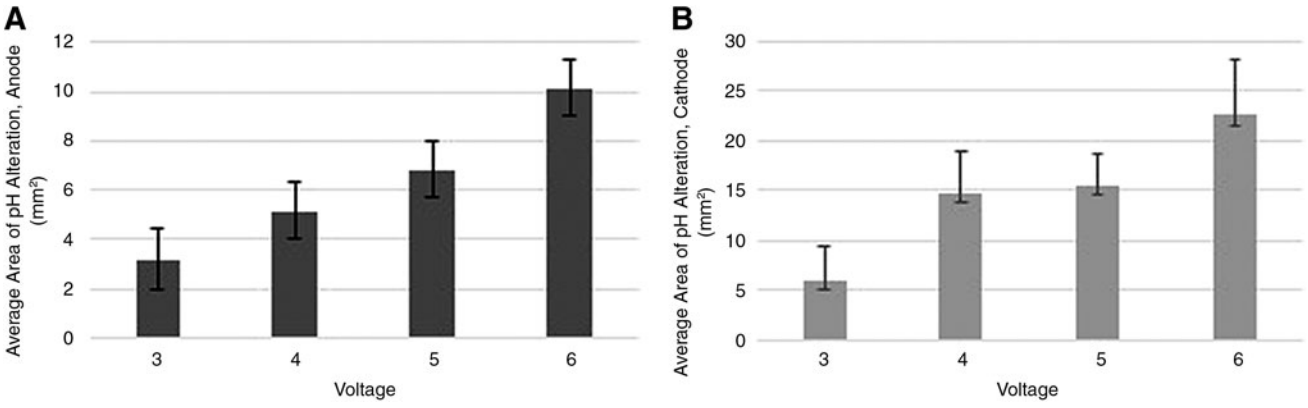

Fig. 4. ECL effect (mm^2) on human adipose tissue at constant time (5 min) and increasing voltage (3 V for 5 min: $n=6$, 4 V for 5 min: $n=10$, 5 V for 5 min: $n=11$, 6 V for 5 min: $n=8$). **(A)** Average area of pH change at anode. **(B)** Average area of pH change at cathode.

pH disturbance generated at the anode compared with the cathode in treatment group 3 V for 5 min (6.04 mm^2 vs. 2.95 mm^2, $p = 0.40$, 95% CI −4.8 to 11]). A significantly greater area of pH disruption was generated at the cathode versus the anode in groups 4 V for 5 min (14.7 mm^2 vs. 5.00 mm^2, $p = 0.032$, 95% CI 0.93–19), 5 V for 5 min (15.5 mm^2 vs. 6.72 mm^2, $p = 0.019$, 95% CI 1.6–16), and 6 V for 5 min (22.5 mm^2 vs. 10.0 mm^2, $p = 0.047$, 95% CI 0.22–25).

Histology

Representative histological images of samples are shown, demonstrating morphology in the subcutaneous layer in both control and ECL-treated tissue (Fig. 5). Well-organized regularly sized adipocytes with clear cytoplasm are seen in control specimens (Fig. 5A, F). Acute structural changes in adipocytes were observed in all specimens, including the retraction of fat lobules and rupture of the adipocyte cytoplasmic membrane. This strongly suggests fat cell destruction, and is observed at anodes and cathodes. The anode site in the 3 V for 5 min ECL group (Fig. 5B) demonstrates the denaturation and shrinkage of the fat lobules with extravasated red blood cells. The cathode site shows fewer cell nuclei. In the 4 V for 5 min ECL group (Fig. 5C, H), dystrophic changes are observed in the fat with more intensified shrinkage and retraction of the fat lobules than seen in the 3 V for 5 min group. The anode site in the 5 V for 5 min ECL group shows collapse of the normal fat lobule configuration, resulting from adipocytic cytoplasmic membrane rupture (Fig. 5D). There is diffuse injury to the fat layer with hemorrhage at the cathode site (Fig. 5I). Structurally compromised fat tissue stains eosinophilic at the anode site in the 6 V for 5 min ECL group (Fig. 5E) and some hyalinization are observed. Vascular damage is prominent at the cathode site (Fig. 5J). Nearby adipocytes are necrotic, with vacuolization of adipocyte nuclei and loss of chromatin.

Discussion

Results from our preliminary study indicate that ECL therapy induced using platinum-based electrode needles can provoke selective damage to ex vivo human fatty tissue. In our protocol, injecting normal saline into adipose tissue to the point of tumescence is critical. Fat tissue is an electrical insulator; untreated adipose tissue restricts the flow of current, limiting hydrolysis, and thus reducing the overall effect of ECL treatment.[18] In contrast, saline conducts electricity, allows current to flow between electrodes, and splits water molecules. ECL injures adipocytes and this effect is spatially limited and dictated by dosimetry. Triglcyerides are likely saponified as well, but this requires techniques that are beyond the scope of this study.

pH mapping revealed an increase in effect area with increasing voltage, suggesting that the dosimetry parameter (along with electrode geometry) may be fine tuned to treat a desired volume of subcutaneous tissue. At each voltage, the area of pH change at the cathode

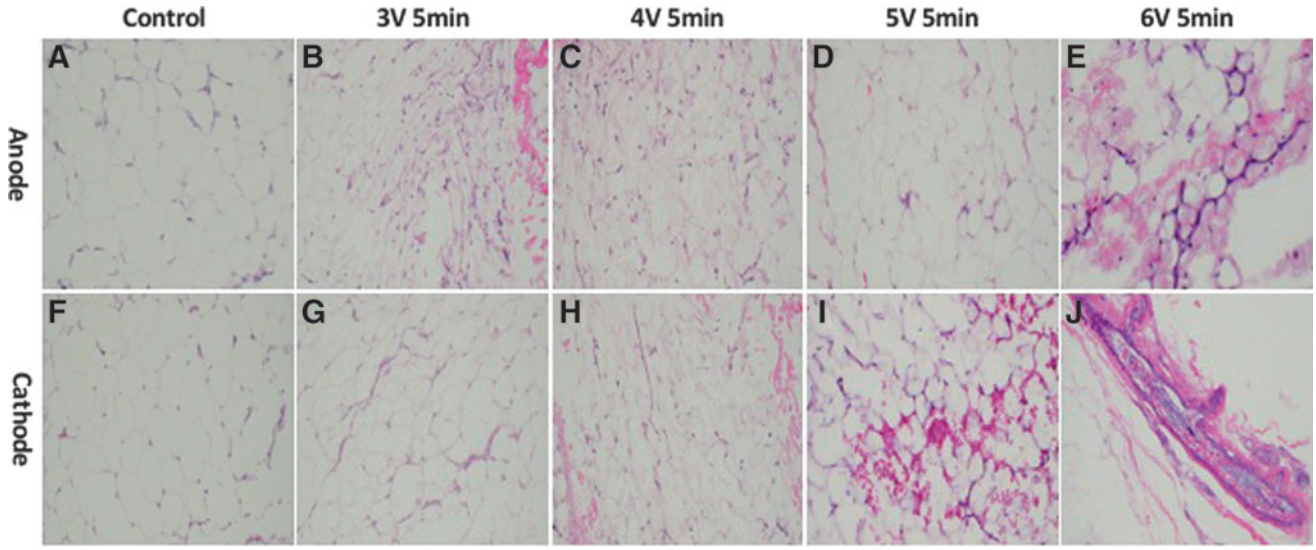

Fig. 5. Hematoxylin and eosin staining of subcutaneous layer. ECL was performed at increasing voltage with a constant duration of 5 min. Representative microscopic fields of untreated control **(A, F)**; anode sites of 3 V **(B)**, 4 V **(C)**, 5 V **(D)**, 6 V **(E)**; and cathode sites of 3 V **(G)**, 4 V **(H)**, 5 V **(I)**, and 6 V **(J)** are depicted. Images are shown at 10× magnification.

(base site) was consistently larger than the anode. This direct acid–base dose–response relationship is consistent with previous studies on electrochemical therapy and is likely due to the generation and migration of chemical species down both their concentration and electropotential gradients.[8,17,19]

Histology

Histological evaluation of control subcutaneous tissue revealed unilocular adipocytes of regular shape and size. A high amount of vascularization was noted within the layer, with multiple capillaries in close contact with each adipocyte. Prior research suggests that death of blood vessels associated with fat tissue leads to targeted apoptosis of bordering adipocytes.[18] In our study, we noted acute vessel damage due to ECL treatment coinciding with adjacent fatty tissue injury. We confirmed loss of adipocyte nuclei at the anode and cathode sites, with rupture of adipocyte membranes, hyalinization, and variation in adipocyte shape and size. Based on these findings, we propose that adipocytes treated with ECL undergo immediate cell death through necrosis rather than apoptosis. Nevertheless, damage to the surrounding blood supply may lead to extended adipocyte destruction over time, and pH-mediated injury to adipocytes may not be evident in ex vivo studies. In vivo, the actual extent of tissue injury may be larger. Future studies are ongoing to explore the long-term therapeutic effects of ECL.

Limitations of our study include the inherent delicate and fragile nature of adipose tissue, which lacks a defined collagen framework. Specimen sectioning is technically difficult and contributes to the nonuniform distribution of the pH dye. We utilized a computational algorithm to better gauge the ROIs and to provide a largely unbiased account of color changes secondary to pH changes. In addition, we were blinded to the clinical history of our patients. Specimens were collected from a heterogeneous patient population who differ in status of weight loss (acute vs. chronic), history of prior bariatric surgery, hormonal status (pre- vs. postmenopausal), age, and overall health at time of surgery. Each of these factors alter adipocyte size and number and can thus influence the therapeutic effect of ECL.[20,21]

This pilot study introduced the acute electrochemical and histopathological effects of ECL on ex vivo human adipose tissue. ECL is a low-cost simple-to-use technology that may serve as a novel minimally invasive outpatient fat reduction therapy. It is important to note that clinical implementation of the technology would utilize a needle-based approach inserted perpendicular or parallel to the surface of the skin, traversing the dermal layer and exposing the electrodes to the dermis. Our nonpublished pilot studies in ex vivo human skin have shown that dermis conducts electricity and we postulate that there is potential for skin injury. Our laboratory is currently developing simple insulating measures at the insertion site to protect the dermal layer during ECL. Further studies are required to optimize needle placement and dermal insulation, investigate the long-term effects of ECL, and better understand the therapeutic value of ECL between heterogeneous adipose tissues. Work in in vivo animal studies as well as needle electrode design is ongoing and will offer further insight into the potential clinical application of ECL.

Conclusions

ECL caused cellular injury in human adipocytes and nearby vessels in ex vivo human adipose tissue. With future development, this technology may offer a low-cost minimally invasive method of destroying adipocytes for medical or cosmetic purposes.

Disclaimer

The content of the article is solely the responsibility of the authors and does not necessarily represent the official views of the NIH.

Author Disclosure Statement

The authors declare no financial interests, activities, relationships, and affiliations with respect to this study.

Funding Information

This research was supported by the Irvine Head and Neck Research Foundation, George Hewett Foundation, LAMMP Grant funded by the National Institutes of Health/National Institute of Biomedical Imaging and Bioengineering (NIH/NIBIB) (Grant No. P41-EB015890), Chao Cancer Center Grant funded by the National Cancer Institute (NIH/NCI) (Grant No. 2P30CA062203-19), and the Leading Foreign Research Institute Recruitment Program through the National Research Foundation of Korea (NRF) funded by the Ministry of Science and ICT (MSIT) (Grant No. NRF-2018K1A4A3A02060572).

Supplementary Material

Supplementary Figure S1

References

1. Sarwer DB, Crerand CE. Body image and cosmetic medical treatments. *Body Image.* 2004;1(1):99–111.
2. Ingargiola MJ, Motakef S, Chung MT, et al. Cryolipolysis for fat reduction and body contouring: safety and efficacy of current treatment paradigms. *Plast Reconstr Surg.* 2015;135(6):1581–1590.
3. Deeks ED. Deoxycholic acid: a review in submental fat contouring. *Am J Clin Dermatol.* 2016;17(6):701–707.
4. Mulholland RS, Kreindel M. Non-surgical body contouring: introduction of a new non-invasive device for long-term localized fat reduction and cellulite improvement using controlled, suction coupled,

radiofrequency heating and high voltage ultra-short electrical pulses. *J Clin Exp Dermatol Res.* 2012;3:4.
5. Avci P, Nyame TT, Gupta GK, et al. Low-level therapy for fat layer reduction: a comprehensive review. *Lasers Surg Med.* 2013;45(6):349–357.
6. Katz B, Bard R, Goldfarb R, et al. Ultrasound assessment of subcutaneous abdominal fat thickness after treatments with a high-intensity focused electromagnetic field device: a multicenter study. *Dermatol Surg.* 2019;45(12):1542–1548.
7. Friedmann D. A review of the aesthetic treatment of abdominal subcutaneous adipose tissue: background, implications, and therapeutic options. *Dermatol Surg.* 2015;41(1):18–34.
8. Protsenko DE, Ho K, Wong BJ. Stress relaxation in porcine septal cartilage during electromechanical reshaping: mechanical and electrical responses. *Ann Biomed Eng.* 2006;34(3):455–464.
9. Chae Y, Protsenko D, Holden PK, et al. Thermoforming of tracheal cartilage: viability, shape change, and mechanical behavior. *Lasers Surg Med.* 2008;40(8):550–561.
10. Manuel CT, Foulad A, Protsenko DE, et al. Needle electrode-based electromechanical reshaping of cartilage. *Ann Biomed Eng.* 2010;38(11):3389–3397.
11. Lim A, Protsenko DE, Wong BJ. Changes in the tangent modulus of rabbit septal and auricular cartilage following electromechanical reshaping. *J Biomech Eng.* 2011;133(9):094502.
12. Manuel CT, Foulad A, Protsenko DE, et al. Electromechanical reshaping of costal cartilage grafts: a new surgical treatment modality. *Laryngoscope.* 2011;121(9):1839–1842.
13. Wu EC, Protsenko DE, Khan AZ, et al. Needle electrode-based electromechanical reshaping of rabbit septal cartilage: a systematic evaluation. *IEEE Trans Biomed Eng.* 2011;58(8):2378–2383.
14. Badran K, Manuel C, Waki C, et al. Ex vivo electromechanical reshaping of costal cartilage in the New Zealand white rabbit model. *Laryngoscope.* 2013;123(5):1143–1148.
15. Oliaei S, Manuel C, Karam B, et al. In vivo electromechanical reshaping of ear cartilage in a rabbit model: a minimally invasive approach for otoplasty. *JAMA Facial Plast Surg.* 2013;15(1):34–38.
16. Moy WJ, Su E, Chen JJ, et al. Association of electrochemical therapy with optical, mechanical, and acoustic impedance properties of porcine skin. *JAMA Facial Plast Surg.* 2017;19(6):502–509.
17. Hu AC, Hong EM, Toubat O, et al. Multiphoton microscopy of collagen structure in ex vivo human skin following electrochemical therapy. *Lasers Surg Med.* 2019; DOI:10.1002/lsm.23094.
18. Kolonin MG, Saha PK, Chan L, et al. Reversal of obesity by targeted ablation of adipose tissue. *Nat Med.* 2004;10(6):625–632.
19. Kuan EC, Hamamoto AA, Manuel CT, et al. In-depth analysis of pH-dependent mechanisms of electromechanical reshaping of rabbit nasal septal cartilage. *Laryngoscope.* 2014;124(10):E405–E410.
20. Franklin RM, Ploutz-Snyder L, Kanaley JA. Longitudinal changes in abdominal fat distribution with menopause. *Metabolism.* 2009;58(4):311–315.
21. Murphy J, Moullec G, Santosa S. Factors associated with adipocyte size reduction after weight loss interventions for overweight and obesity: a systematic review and meta-regression. *Metabolism.* 2017;67:31–40.